ISSN 0001-4338, Izvestiya, Atmospheric and Oceanic Physics, 2018, Vol. 54, No. 8, pp. 848–858. © Pleiades Publishing, Ltd., 2018.
Original Russian Text © Yu.F. Kopnichev, I.N. Sokolova, 2018, published in Geofizicheskie Protsessy i Biosfera, 2018, Vol. 17, No. 1, pp. 109–124.

Ring-Shaped Seismicity Structures Forming before Large Earthquakes and the Great Earthquakes in the Western and Eastern Pacific

Yu. F. Kopnichev[a], * **and I. N. Sokolova**[b], **

[a] *Schmidt Institute of Physics of the Earth, Russian Academy of Sciences, Moscow, 123242 Russia*
[b] *Institute of Geophysical Research, Ministry of Energy of the Republic of Kazakhstan, Almaty, 050020 Kazakhstan*
**e-mail: yufk777@mail.ru*
***e-mail: sokolova.inessa@mail.ru*

Abstract—We consider the characteristics of seismicity before large earthquakes and the great earthquakes in the periphery of the Pacific Ocean. It is found that earthquakes with M_w = 7.0–9.2 that occurred in 1964–2016 were preceded by the formation of ring-shaped seismicity structures, usually in two depth ranges: 0–33 and 34–70 km. We obtain correlations between sizes of shallow (L) and deep (l) seismicity rings, threshold magnitudes (M_{th1} and M_{th2}, respectively), and the time of their formation (T_1 and T_2, respectively) on magnitudes M_w of the mainshocks. It is shown that the sizes of ring-shaped structures at any given M_w for earthquakes in the western margin of the Pacific are significantly smaller than for those in the eastern margin. However, the values of M_{th1} and M_{th2} are close for these two regions. Parameters T_1 and T_2 vary considerably depending on the event, but on average they are ~27–30 years. It is supposed that the formation of ring-shaped structures is related to the migration of deep-seated fluids, while the difference between characteristics of these structures in the western and eastern margins of the Pacific are caused by different contents of fluids in the crust and upper mantle of the respective regions. This conclusion agrees with the available data on the peculiarities of aftershock processes of large earthquakes in the considered regions.

Keywords: ring-shaped seismicity structures, large earthquakes, lithosphere, deep-seated fluids

DOI: 10.1134/S0001433818080054

INTRODUCTION

In the last 10 years the authors have obtained a lot of data indicating the formation ring-shaped structures of seismicity before large earthquakes and largest earthquakes in different subduction zones (Kopnichev and Sokolova, 2009a–2009c, 2010, 2011a, 2011b, 2015). The analysis of characteristic of these structures allowed us, in particular, to forecast the locations and magnitudes of the catastrophic Tohoku earthquake (M_w = 9.0, March 11, 2011, offshore northeast Japan) and the great earthquake, Ikike (M_w = 8.2, April 1, 2014, Chile) (Kopnichev and Sokolova, 2009c, 2011a, 2015). To enhance the accuracy of forecasting the locations and energies of great earthquakes, the regional peculiarities of ring-shaped structures should be revealed. In the present work, we consider the characteristics of ring-shaped structures in the western and eastern Pacific.

HISTORICAL SEISMICITY

Western Pacific

The region under consideration extended from New Zealand to Kamchatka and the western Aleutian Islands (to the west of 180° E). Beginning from 1900, more than 20 shallow (h < 50 km) earthquakes with $M_w \geq 8.0$ occurred in this region (Engdahl and Villasenor, 2002). The largest of them were the Great Kamchatka earthquake (November 4, 1952, M_w = 9.0) and the catastrophic Tohoku one (March 11, 2011, M_w = 9.0). Both earthquakes generated powerful tsunamis that traveled across the entire Pacific Ocean. The Tohoku earthquake was completely unexpected by Japanese seismologists who, proceeding from historical and geophysical data, did not believe that such a large event could occur in this region. After a revision of available data, it was concluded that the recurrence period T_r for earthquakes of close magnitudes was ~800–1200 years (Goldfinger et al., 2013).

Eastern Pacific

We analyzed the characteristics of seismicity in different subduction zones between central Chile and eastern Aleutian Islands (to the east of 180° E). The number of large earthquakes with $M_w \geq 8.0$ that occurred here beginning from 1900 is also more than 20, including the Great Chilean earthquake (May 22, 1960, M_w = 9.6) and the Great Alaskan one (March 28, 1964, M_w = 9.2), which had been the largest instrumentally recorded seismic events in the world (Engdahl and Villasenor, 2002). Both these earthquakes caused giant tsunamis which, however, did not take death tolls comparable to the tsunami generated by the Tohoku earthquake of March 11, 2011.

Thus, the reported maximal magnitudes of these earthquakes are bigger in the eastern Pacific than in the western one.

DATA AND METHODS

Analogously to our earlier publications (Kopnichev and Sokolova, 2009a, 2009b, 2010, 2011a, 2011b), we considered the characteristics of seismicity in the study area that included the rupture zone of the large earthquake. We made the maps of earthquake epicenters for two depth ranges, 0–33 and 34–70 km, tending to use the data starting from 1964, when the coordinates of earthquakes began to be determined quite accurately owing to the appearance of the Worldwide Standardized Seismographic Network, WWSSN (Butler et al., 2004). We analyzed the data from seismic catalogs of the National Earthquake Information Center, United States Geological Survey (NEIC USGS), beginning from 1973, and the International Seismological Centre (ISC) for the period of 1964–1972 (with the only exclusion of the Great Alaskan earthquake, for which the range of analyzed data was 1938–1964).

The technique of distinguishing ring-shaped seismicity structures is characterized by the following peculiarities.

(1) The duration of the period for which the characteristics of seismicity are studied is about 40 years, and this corresponds to the maximal values reported by present.

(2) The parameters of seismicity are considered for two depth ranges, 0–33 and 34–70 km, where ring-shaped structures form. The seismic events selected for each depth range have magnitudes equal to or higher than the threshold value of the given depth range (M_{th1} and M_{th2}, respectively), and these values are usually lower than the magnitude of the mainshock by 2–3 magnitude units.

(3) The values of threshold magnitudes M_{th} are adjusted for both depth ranges in order to find the optimal values at which ring-shaped structures are distinguished the most clearly. This procedure is exemplified in Fig. 1, where the case of the large earthquake in Peru (November 12, 1996, $M_w = 7.7$) is considered. It is seen from Fig. 1a that, at $M_{th1} = 4.8$, the shallow NW-elongated (major axis is ~160-km-long) ring-shaped structure is manifested quite distinctly. At a lower threshold magnitude ($M_{th1} = 4.7$), this ring-shaped structure becomes vaguer (Fig. 1b) and only rings of smaller size can be distinguished. At a higher threshold magnitude ($M_{th1} = 4.9$), the seismicity ring disappears and only linear structures can be distinguished (Fig. 1c).

(4) Ring-shaped structures are usually approximated by ellipses. Seismicity rings are constructed in a way that an approximately equal number of relatively weak events are located on both sides of the contours of ellipses. A seismicity ring is considered formed if the maximal width of the band of epicenters that form it (the sum of maximal deviations of epicenters located within and beyond the ellipse, relative to its contour) does not exceed 1/4 of the length of ellipse's minor axis (criterion of the ring structure quality). Epicenters marked in Fig. 1a satisfy this criterion.

(5) Ring-shaped structures having the largest possible values of M_{th1} and M_{th2} are selected. Proceeding from the earlier data (Kopnichev and Sokolova, 2009a–2009c, 2010, 2011a, 2011b, 2015), we consider the deep structures crossing or almost touching shallow ones. Everything else being equal, the selected seismicity ring has the longest major axis of ellipse (L and l for the shallow and deep ring, respectively).

(6) The parameters of seismicity need to be controlled on a regular basis (at least once every half of a year), because there have been cases reported when new ring structures with greater values of M_{th} formed in 1–2 years; for example, this occurred before the Tohoku earthquake of March 11, 2011 (Kopnichev and Sokolova, 2011a).

DATA ANALYSIS

Western Pacific

Figure 2 presents data on seismicity in the region of northeast Japan before the Tohoku earthquake of March 11, 2011. It can be seen that ring-shaped structures with relatively high threshold magnitudes formed: shallow one, NE-oriented ($M_{th1} = 5.9$, $L \sim 140$ km) and deep one stretching along 142° E ($M_{th2} = 5.4$, $l \sim 75$ km). The formation periods of these structures were $T_1 = 30$ and $T_2 = 35$ years, respectively. The largest M_w magnitudes of earthquakes occurring within the limits of these structures were reported to be 7.0 (July 19, 2008) and 7.7 (June 12, 1978), respectively. Importantly, the epicenter of the Tohoku earthquake was located at the eastern intercept of the seismicity rings (i.e., in the nearest vicinity of the point of intercept of ellipses approximating these structures).

Table 1 contains the data on parameters of ring-shaped structures formed in the western Pacific.

Figure 3 presents the dependence of the sizes of shallow rings on the magnitudes of mainshocks for this region. The value of L grows with an increase in M_w (although quite weakly) and the equation of linear regression is of the following form:

$$\log L(\text{km}) = 0.25 + 0.21M_w,\ r = 0.68, \quad (1)$$

where r is the correlation factor.

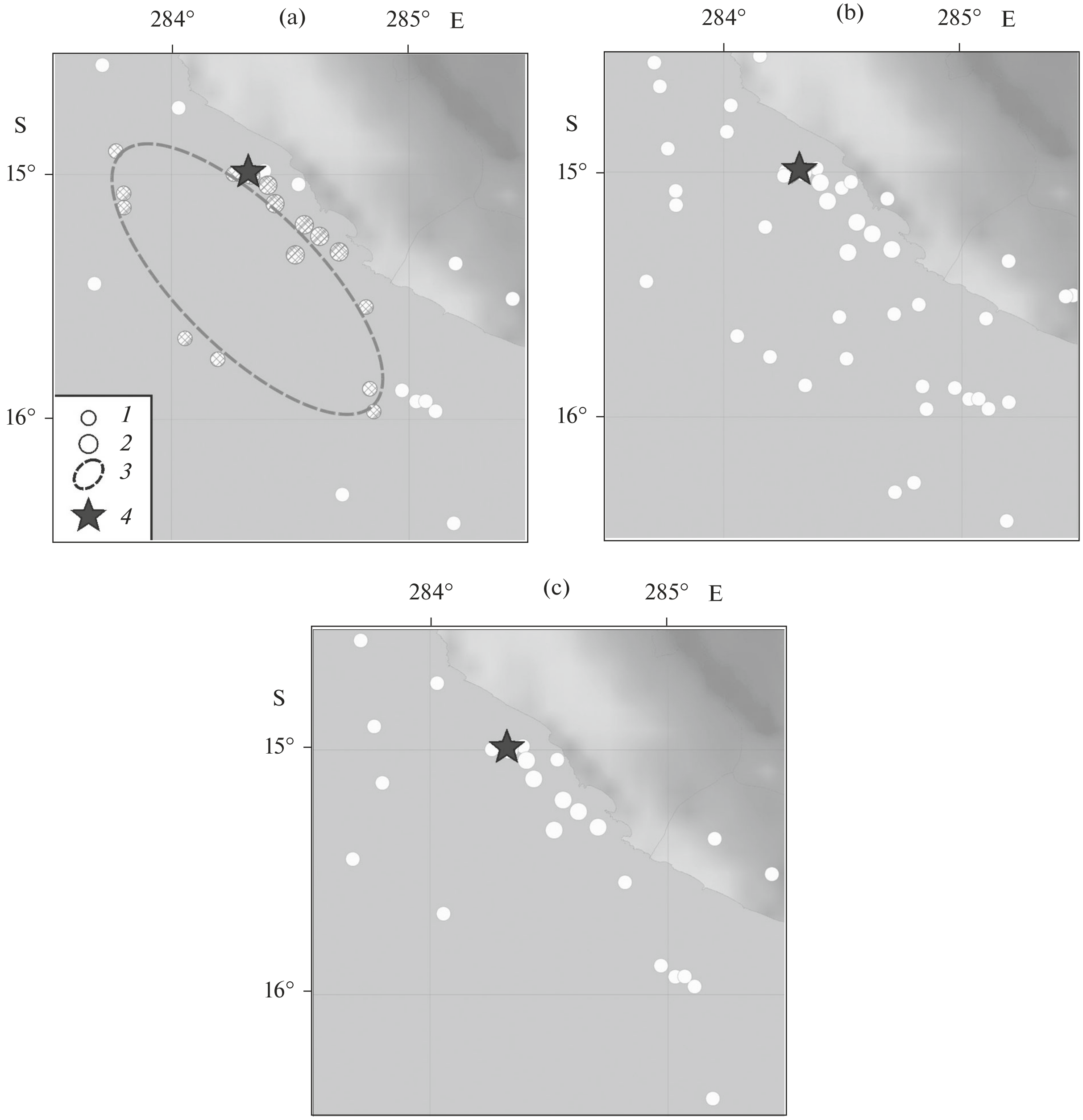

Fig. 1. Example of distinguishing the shallow ring-shaped structure formed prior to the Peruvian earthquake of November 12, 1996. (a) $M_{\text{th1}} = 4.8$; earthquake epicenters ($h = 0$–33 km): (*1*) $M < 5.5$, (*2*) $M \geq 5.5$ (hatched circles denote the epicenters that formed the seismicity ring), (*3*) ring-shaped structure, and (*4*) mainshock ($M_w = 7.7$) epicenter; (b) $M_{\text{th1}} = 4.7$; and (c) $M_{\text{th1}} = 4.9$.

It follows from Fig. 4 that the values of M_{th1} quickly grow with the increase in M_w; the equation of linear regression is described by the following formula:

$$M_{\text{th1}} = -1.88 + 0.85M_w,\ r = 0.89. \quad (2)$$

Figure 5 illustrates the regional dependence of the time of the formation of the shallow seismicity ring on magnitude. One can see that there is a weak growth of T_1 in the background of quite a large scatter of data. The following correlation dependence was obtained:

$$T_1\,(\text{years}) = 5.83 + 2.96M_w,\ \ r = 0.27. \quad (3)$$

Figure 6 shows the regional dependence of the sizes of deep rings on M_w magnitudes. In this case, values of l show almost no dependence on magnitude, and the equation of linear regression is characterized by a very low correlation factor:

$$\log l\ (\text{km}) = 1.31 + 0.07\ M_w,\ \ r = 0.27. \quad (4)$$

However, the values of M_{th2}, as well as those of M_{th1}, grow quite quickly with the increase in M_w (Fig. 7). The

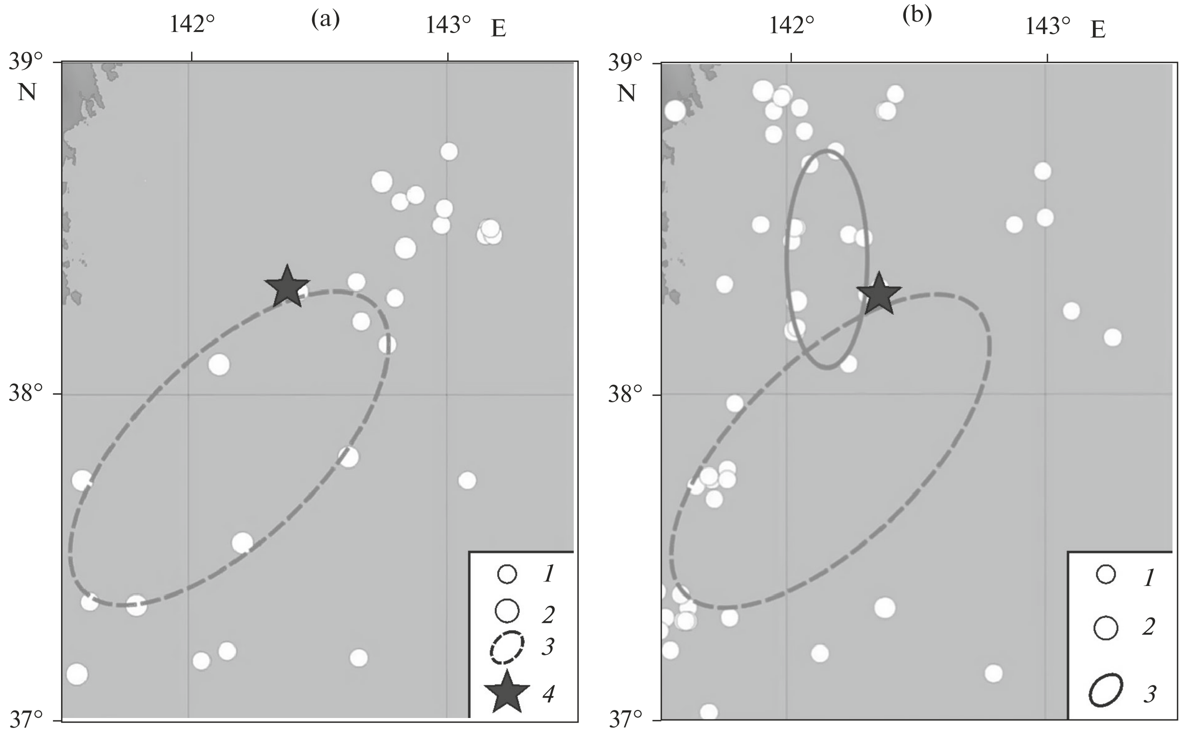

Fig. 2. Characteristics of seismicity before the Tohoku earthquake of March 11, 2011, for hypocentral depths of (a) 0–33 and (b) 34–70 km. Notations for panel (a): (*1*, *2*) epicenters of earthquakes with (*1*) $5.9 \leq M < 6.5$ and (*2*) $M \geq 6.5$; (*3*) shallow ring and (*4*) mainshock ($M_w = 9.0$) epicenter. Notations for panel (a): (*1*, *2*) epicenters of earthquakes with (*1*) $5.4 \leq M < 6.5$ and (*2*) $M \geq 6.5$; (*3*) deep ring. The rest of the notations are the same as in panel (a).

following equation of linear regression with a very high correlation factor was obtained:

$$M_{\text{th2}} = -0.95 + 0.70\ M_w,\ \ r = 0.94. \qquad (5)$$

The values of both T_2 as T_1 demonstrate a large scatter of data (Fig. 8); the correlation dependence is of the following form:

$$T_2\ (\text{years}) = 7.14 + 2.89M_w,\ \ r = 0.20. \qquad (6)$$

Note that mean values of T_1 and T_2 for the western Pacific are 28.7 ± 6.1 and 29.5 ± 8.2 years, respectively.

Eastern Pacific

Figure 9 shows the data on seismicity in the considered region before the Adak earthquake of May 7, 1986 ($M_w = 8.0$), which occurred in the western flank of the

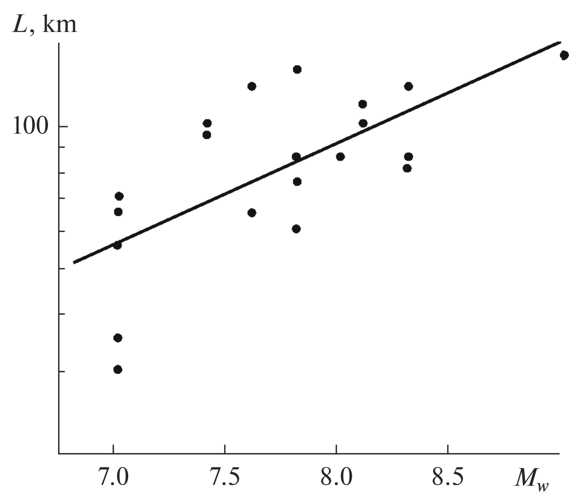

Fig. 3. $\log L(M_w)$ dependence for the western Pacific.

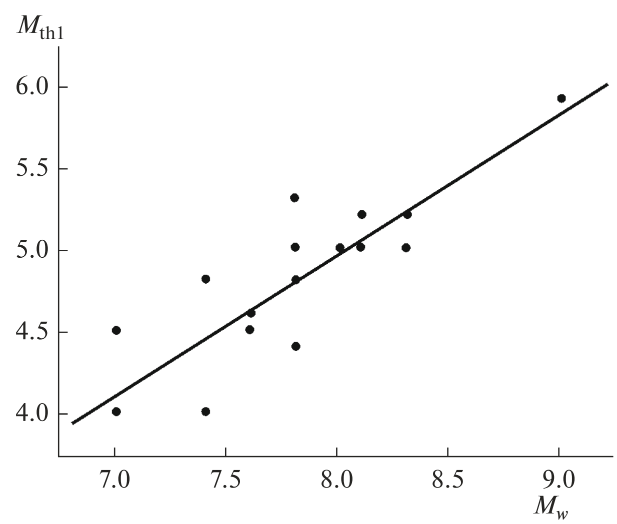

Fig. 4. $M_{\text{th1}}(M_w)$ dependence for the western Pacific.

Table 1. Characteristics of ring-shaped structures formed prior to large earthquakes in the western Pacific

Date, dd.mm.yyyy	M_w	L, km	M_{th1}	T_1, yrs	l, km	M_{th2}	T_2, yrs	Region
01.11.1989	7.4	100	4.0	18	95	4.0	18	Northeast Japan
13.11.1993	7.0	70	4.5	19	80	4.0	17	South Kamchatka
04.10.1994	8.3	80	5.0	25	80	5.1	27	Northeast Japan
28.12.1994	7.8	130	4.4	23	85	4.4	21	Northeast Japan
05.12.1997	7.8	85	5.3	24	75	4.5	23	Kamchatka Pen.
25.09.2003	8.3	85	5.0	28	40	5.0	29	Northeast Japan
31.10.2003	7.0	30	4.0	17	40	4.0	26	Northeast Japan
17.11.2003	7.8	75	4.8	30	70	4.6	32	West Aleutian Islands
28.11.2004	7.0	65	4.0	31	40	3.9	31	Northeast Japan
15.11.2006	8.3	120	5.2	31	90	4.7	33	Kuril Islands
13.01.2007	8.1	100	5.2	30	50	4.5	30	Kuril Islands
19.07.2008	7.0	55	4.0	34	40	4.0	35	Northeast Japan
15.01.2009	7.4	95	4.8	28	80	4.2	18	Kuril Islands
19.03.2009	7.6	120	4.6	33	55	4.4	19	Tonga Islands
29.09.2009	8.1	110	5.0	34	110	4.8	34	Samoa Islands
11.03.2011	9.0	140	5.9	30	75	5.4	35	Northeast Japan
06.07.2011	7.6	65	4.5	35	80	4.7	35	Kermadek Islands
06.02.2013	8.0	85	5.0	37	70	4.7	40	Santa Cruz Islands
01.09.2016	7.0	35	4.0	29	85	4.1	43	New Zealand
08.12.2016	7.8	60	5.0	38	100	4.7	43	Solomon Islands

zone where the great earthquake occurred in 1957 (Engdahl and Villasenor, 2002). It follows from the data presented in Fig. 9 that this earthquake was also preceded by the formation of seismicity rings: the shallow one had $M_{th1} = 4.8$, $L \sim 260$ km, and $T_1 = 22$ years, while the deep one had $M_{th2} = 4.7$, $l \sim 85$ km, and $T_2 = 16$ years. The maximal magnitudes of earthquakes within the limits of these rings are 6.1 and 6.3, respectively. Both rings are elongated in sublatitudinal direction, with the mainshock epicenter being located at about 40 km from the intercept of rings, and this is multiple times less than the size of the shallow ring. Note that in some cases shallow and deep ring-shaped structures do not intercept or even touch, but are

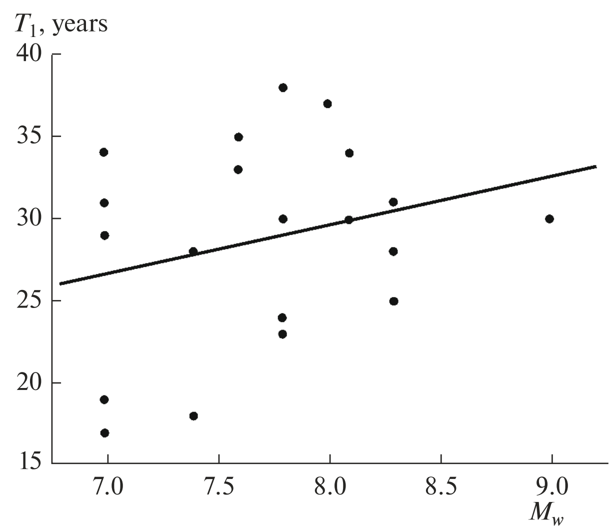

Fig. 5. $T_1(M_w)$ dependence for the western Pacific.

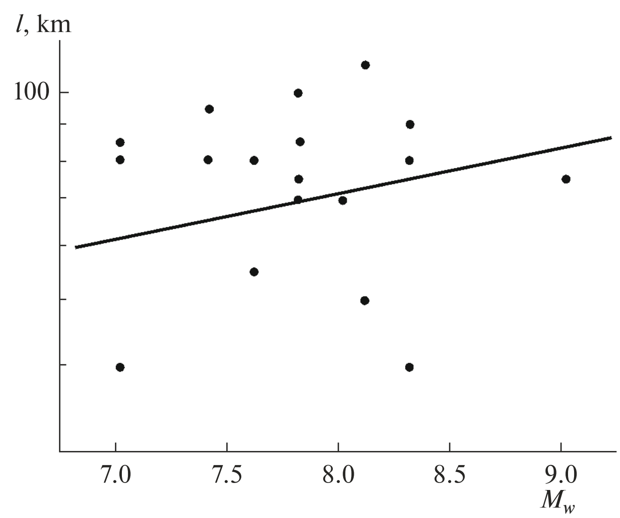

Fig. 6. log$l$ (M_w) dependence for the western Pacific.

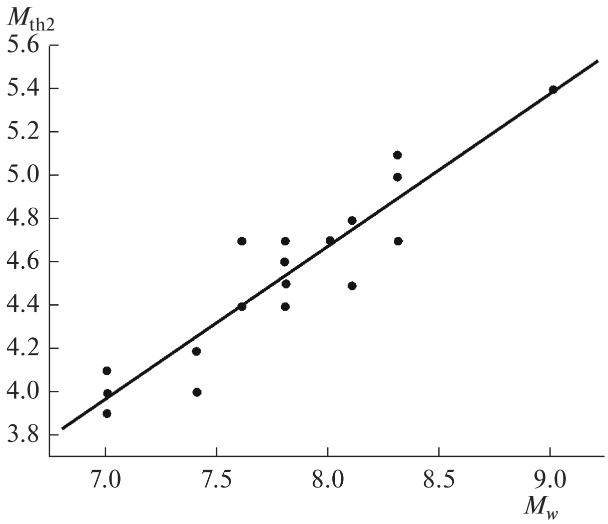

Fig. 7. $M_{th2}(M_w)$ dependence for the western Pacific.

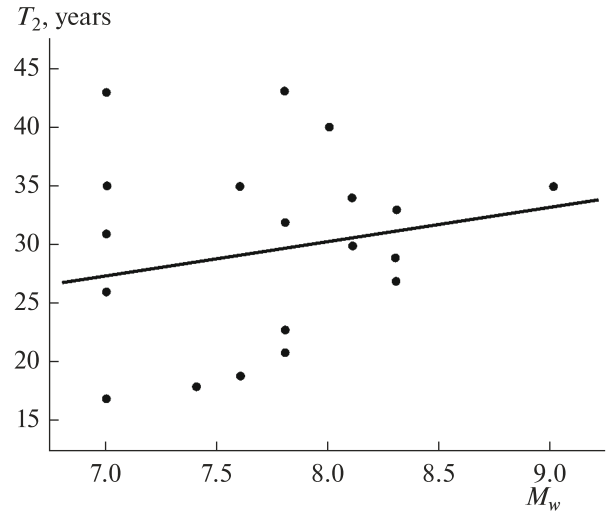

Fig. 8. $T_2(M_w)$ dependence for the western Pacific.

located at some distance from each other and this distance is much less than sizes of both rings—for example, before the Maule earthquake of February 27, 2010 ($M_w = 8.8$), in Chile (Kopnichev and Sokolova, 2011b).

Table 2 lists the data on parameters of ring-shaped structures in the eastern Pacific.

Figure 10 presents the log$L$ (M_w) dependence for the eastern Pacific. In this case, we can see a rapid growth in parameter L with the increase in magnitude of the mainshock; the equation of linear regression is of the following form:

$$\log L\ (\text{km}) = -1.22 + 0.44\ M_w,\ \ r = 0.86. \quad (7)$$

For the magnitude range of $M_w = 7.0$–9.2, values L in the eastern Pacific grow with the increase in M_w much more quickly than in the western Pacific; hence, at $M_w = 9.0$ the difference between values of log$L$ for these two regions reaches ~0.55 logarithmic units.

Figure 11 shows the M_{th1} (M_w) dependence for the eastern Pacific. The values of M_{th1} quickly grow with the increase in magnitude M_w; however, there is a tendency toward a decrease in slope angle at M_w ~> 8.0. For the entire set of data, the equation of linear regression is described by the following formula:

$$M_{th1} = -0.23 + 0.63\ M_w,\ \ r = 0.88. \quad (8)$$

In this case, the slope of the regression line is slightly less than for the western Pacific.

The values of T_1 in the eastern Pacific demonstrate a weak growth with the increase in magnitude (Fig. 12). The equation of linear regression is described by the following formula:

$$T_1\ (\text{years}) = -9.11 + 4.72\ M_w,\ \ r = 0.32. \quad (9)$$

The analogous dependences for deep rings are presented in Figs. 13–15. The data presented in Fig. 13 suggest that, in contrast to the western Pacific, parameter l in the eastern Pacific demonstrates a relatively fast growth with M_w; the equation of linear regression is of the following form:

$$\log l\ (\text{km}) = -1.16 + 0.40\ M_w,\ \ r = 0.88. \quad (10)$$

Note that deep ring-shaped structures have not been identified in the eastern Pacific, namely, in the Cascadia subduction zone, or in the regions of Mexico and Ecuador (Table 2).

Figure 14 illustrates the M_{th2} (M_w) dependence for the eastern Pacific; it appears to be quite close to that for the western Pacific. The following equation of linear regression was obtained:

$$M_{th2} = -0.80 + 0.69\ M_w,\ \ r = 0.86. \quad (11)$$

The $T_2(M_w)$ correlation dependence obtained in the background of a large scatter of data (Fig. 15) is described by the following formula:

$$T_2\ (\text{years}) = -22.23 + 6.36\ M_w,\ \ r = 0.48. \quad (12)$$

Hence, parameters T_1 and T_2 grow with the increase in magnitude more quickly in the eastern Pacific when compared the western one. Mean values of T_1 and T_2 in the eastern Pacific are 27.3 ± 8.4 and 27.4 ± 7.8 years, respectively, and these are slightly less than for the western Pacific.

It follows from the formulas given above that, excluding the value of l for the western Pacific, there are relatively high correlation factors for dependences of ring sizes and threshold magnitudes on the magnitudes of mainshocks. However, the correlation between values T_1, T_2, and M_w is very weak.

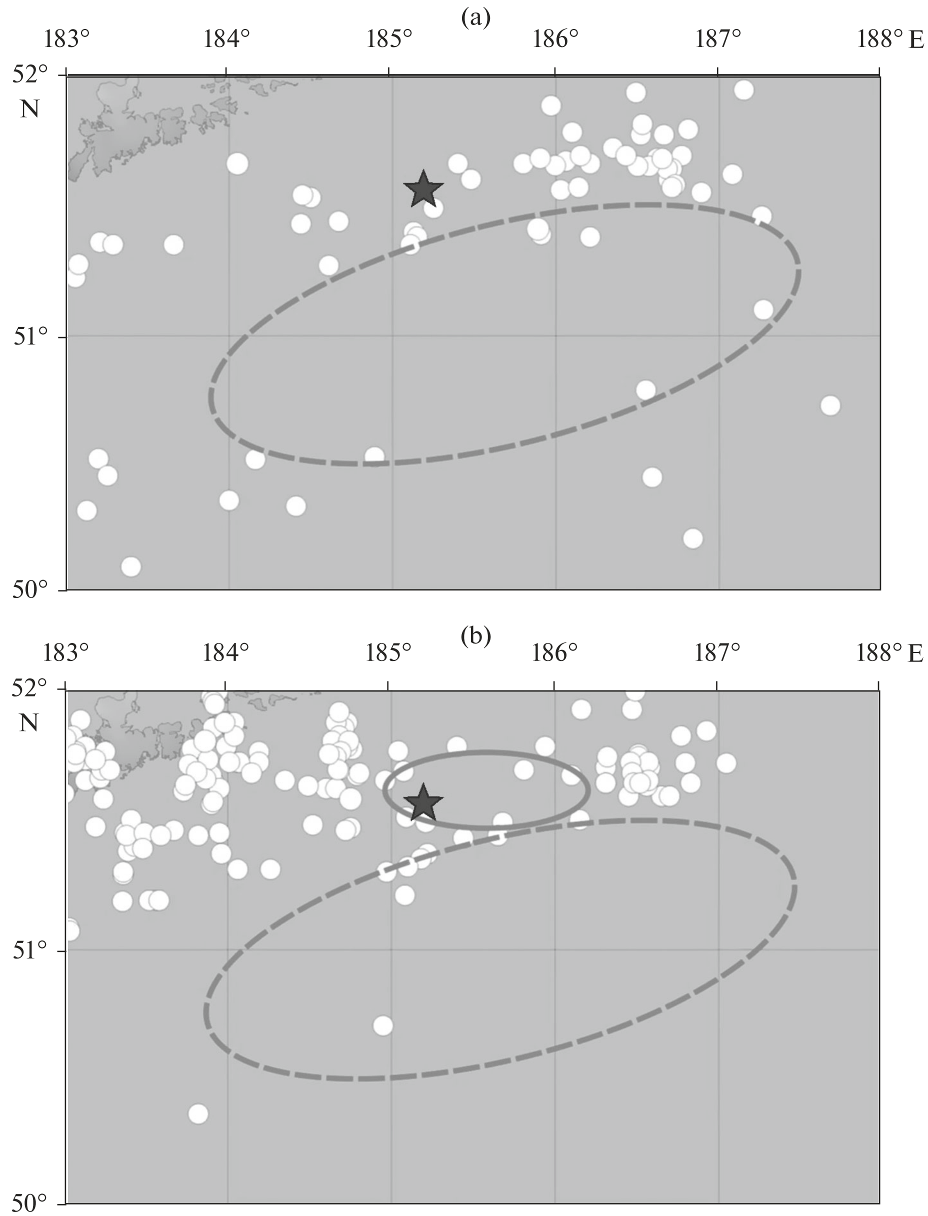

Fig. 9. Characteristics of seismicity before the Adak earthquake of May 7, 1986, for hypocentral depths and magnitudes of (a) 0–33 km, $4.8 \le M \le 6.1$, and (b) 34–70 km, $4.7 \le M \le 6.3$. Notations are the same as in Fig. 2.

DISCUSSION

These data indicate that ring-shaped seismicity structures form in most cases within the limits of two depth ranges before large earthquakes and the great earthquakes in the subduction zones in the periphery of the Pacific Ocean. Analogously to the region of Sumatra (Kopnichev and Sokolova, 2009b), main-shock epicenters are usually located near the intercepts or in the zones of maximal proximity of the respective shallow and deep rings.

It was shown in (Kopnichev and Sokolova, 2010, 2011b) that the lower crust and uppermost mantle within the limits of shallow seismicity rings demonstrate lower attenuation of short-period *S*-waves, while higher attenuation is reported at the boundaries of these rings. In contrast, deep seismicity rings correspond to higher attenuation in the upper mantle (Kopnichev and Sokolova, 2011b). The fact that seismicity rings are situated at considerable distances from volcanic regions allows us to believe that the strong attenuation of *S*-waves is caused by relatively high fluid content rather than presence of partially molten rocks (Kopnichev and Sokolova, 2010, 2011b). If fluids form a well-connected network, stresses begin to concentrate at the top of the two-phase layer (Karakin and Lobkovskii, 1982; Gold and Soter, 1984/1985). The

Table 2. Characteristics of ring-shaped structures that formed prior to large earthquakes in the eastern Pacific

Date, dd.mm.yyyy	M_w	L, km	M_{th1}	T_1, yrs	l, km	M_{th2}	T_2, yrs	Region
28.03.1964	9.2	900	5.5	26	450	5.5	32	Alaska
07.05.1986	8.0	260	4.8	22	85	4.7	16	Aleutian Is.
17.08.1991	7.1	60	4.4	17	–	–	–	Cascadia
30.07.1995	8.0	200	5.0	28	100	5.0	19	Chile
03.10.1995	7.0	110	4.0	22	–	–	–	Ecuador
09.10.1995	8.0	160	4.8	22	–	–	–	Mexico
21.02.1996	7.5	120	4.4	23	95	4.3	23	Peru
10.06.1996	7.9	100	5.1	25	65	4.0	26	Aleutian Is.
12.11.1996	7.7	160	4.8	22	110	4.5	23	Peru
30.01.1998	7.1	55	4.5	21	35	4.0	25	Peru
04.08.1998	7.2	85	4.0	13	–	–	–	Ecuador
06.12.1999	7.0	90	4.0	29	70	4.0	26	Alaska
13.01.2001	7.7	140	4.5	26	70	4.5	27	Salvador
23.06.2001	8.4	280	5.0	31	110	5.2	33	Peru
07.07.2001	7.6	50	4.7	13	85	4.0	28	Peru
22.01.2003	7.6	160	4.8	28	–	–	–	Mexico
15.11.2004	7.2	90	4.2	31	55	4.2	13	Colombia
15.08.2007	8.0	170	5.0	34	65	5.0	32	Peru
14.11.2007	7.7	140	4.7	34	70	4.7	34	Chile
19.12.2007	7.2	55	4.0	37	45	4.1	34	Aleutian Is.
27.02.2010	8.8	320	5.0	46	270	5.0	41	Chile
01.04.2014	8.2	220	5.0	37	110	4.9	41	Chile
14.10.2014	7.3	160	4.5	41	50	4.4	21	Salvador

value of excessive stresses is proportional to the thickness of the two-phase layer, giving ground to the explanation of why epicenters of large earthquakes are close to the intercepts or zones of maximal approach of the shallow and deep rings. The fact that ring-shaped structures can be at some distance from each other, without an intercept, can be explained by the fact that the respective fluid fields can be joined in the lower crust, which in seismoactive regions is characterized by the highest fluid content (Van'yan and Hyndman, 1996).

There is a reason to think that the formation of ring-shaped structures reflects the processes of self-

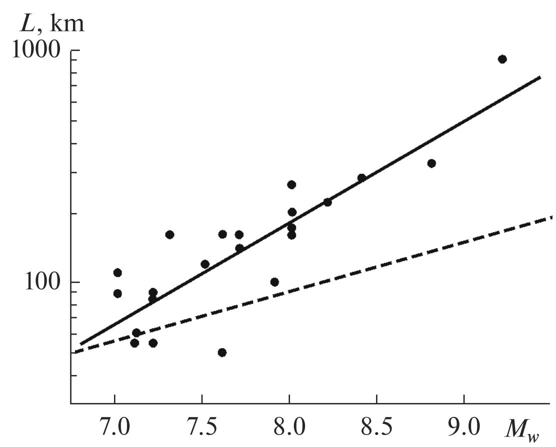

Fig. 10. $\log L(M_w)$ dependence for the eastern Pacific. Dashed line here and in Figs. 11–15 denotes the same dependence for the Western Pacific.

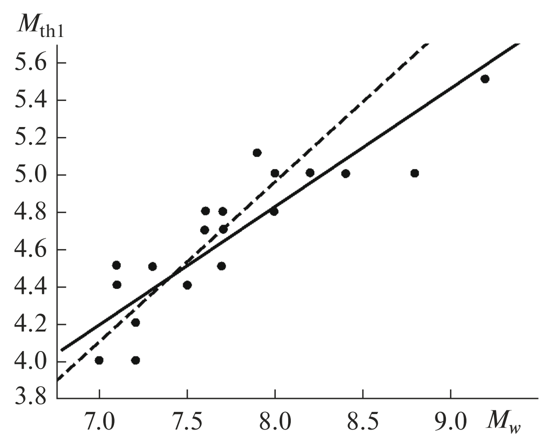

Fig. 11. $M_{th1}(M_w)$ dependence for the eastern Pacific.

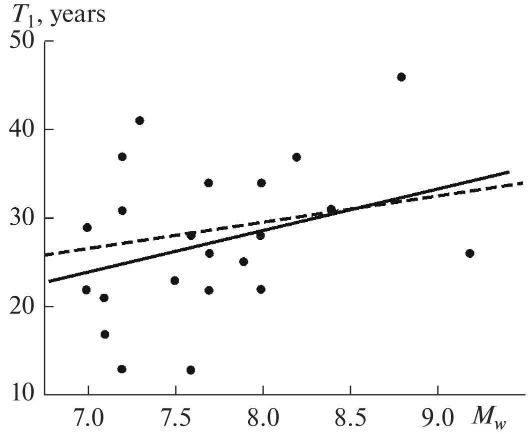

Fig. 12. $T_1(M_w)$ dependence for the eastern Pacific.

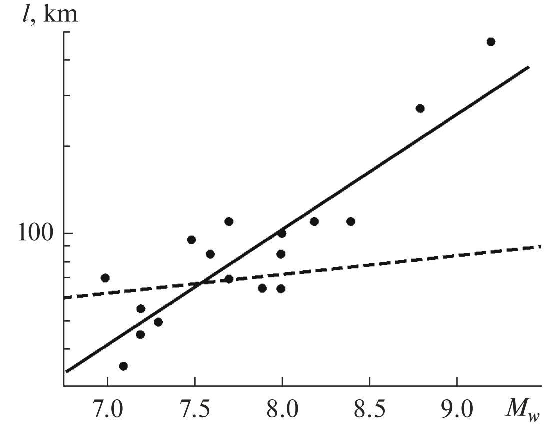

Fig. 13. $\log l(M_w)$ dependence for the eastern Pacific.

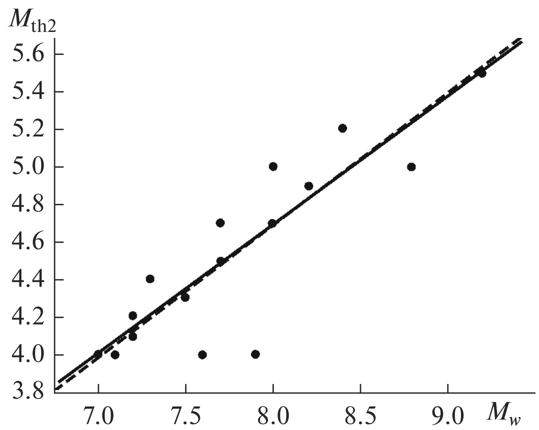

Fig. 14. $M_{th2}(M_w)$ dependence for the eastern Pacific.

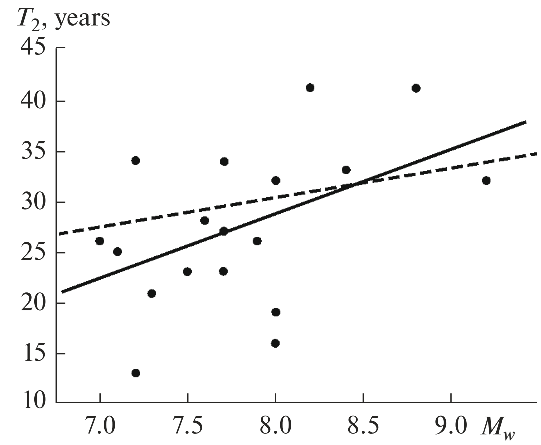

Fig. 15. $T_2(M_w)$ dependence for the eastern Pacific.

organization of geological systems (Letnikov, 1992): these processes cause the ascent of deep fluids, which eventually leads to a decrease in the potential energy of the Earth. It has been found in the last decades that velocities of S-waves in the uppermost mantle after large earthquakes increase (Husen and Kissling, 2001), while attenuation decreases (Kopnichev and Sokolova, 2003; Kopnichev et al., 2009). Additionally, an analysis of literature data shows that the fraction of the mantle helium (^3He) component increases in both rupture zones and their vicinities (Kopnichev and Sokolova, 2005). After the Sumatra–Andaman earthquake of December 26, 2004 (M_w = 9.0), the slow postseismic restoration of geoid depression, probably because of the diffusion of the mantle water, was revealed from gravimetric data (Ogawa and Heki, 2007). All these data obtained by different geophysical and geochemical methods support the idea about the ascent of deep fluids from the uppermost mantle to the crust.

Our results here indicate that the sizes of both shallow and deep rings are generally bigger in the eastern Pacific than in the western Pacific. However, values of threshold magnitudes for the given energy of the mainshock are close for ring-shaped structures in both studied regions of the Pacific. As a possible explanation for these effects, we can suppose that the energy of a large earthquake is proportional to the potential energy of fluids concentrated in the zones of seismicity rings. In this case, smaller seismicity rings in the western Pacific are to be compensated by a higher specific fluid content in the zones of ring-shaped structures of this region. An analogous effect has been revealed earlier for large intracontinental earthquakes with different focal mechanisms (Kopnichev and Sokolova, 2013). In turn, the higher fluid content is explained by the generally older age of the oceanic lithosphere in the western Pacific when compared to the eastern Pacific (Müller et al., 2008; Abers et al., 2013). As is known, the younger subducting lithosphere contains fewer hydrated rocks. Dehydration releases water, which is one of the main components of deep fluids (Yamazaki and Seno, 2003; Abers et al., 2013). In this respect, we should emphasize that the subduction zones of the eastern Pacific, where no deep ring-shaped structures were identified (Cascadia, Mexico, and Ecuador), are remarkable in that the oceanic plates (lithosphere) subducting there are very young, usually less than 10 Ma (Müller et al., 2008; Abers et al., 2013).

The new data correlate with the earlier results of an analysis of aftershock processes in subduction zones in the Pacific periphery. It was shown in (Singh and Suarez, 1988) that the number of aftershocks of large earthquakes, everything else being equal, is considerably larger for seismic events in the western Pacific when compared to the eastern Pacific. In addition, F. Tajima and H. Kanamori (1985) found that the aftershock zones of large earthquakes tend to spread more intensively in the western Pacific when compared to the eastern Pacific. In our opinion, these effects can be related to the following. In the last 10–20 years, the data indicate that fluids in subduction zones ascend from the upper mantle mainly owing to earthquakes (Husen and Kissling, 2001; Yamazaki and Seno, 2003; Kopnichev and Sokolova, 2005; Ogawa and Heki, 2007; Kopnichev et al., 2009). In this respect, a large number of aftershocks (including quite strong ones) provides better "draining" of the fluid-saturated upper mantle in the western Pacific, while in the eastern Pacific, where the upper mantle is less fluid-saturated, the ascent of fluids takes less aftershocks to occur.

Moreover, a bigger expansion of the aftershock zones in the western Pacific is most likely caused by more intensive horizontal migration of fluids that reached the earth's crust. These effects have earlier been revealed for rupture zones of several large intracontinental earthquakes (Rojstaczer and Wolf, 1992; Kopnichev and Sokolova, 2004, 2005).

Thus, the significant difference between sizes of ring-shaped structures in the western and eastern Pacific can be attributed to variations in fluid contents in the crust and upper mantle beneath the respective regions. Note that this conclusion can be verified by analyzing the characteristics of attenuation field of short-period *S*-waves in different subduction zones (Kopnichev and Sokolova, 2011b); another publication will be dedicated to this problem.

At the same time, judging by the available data, the values of T_1 and T_2 depend weakly on the magnitude and the region under study. Note that close mean values of T_1 (~25 ± 5 years) were obtained for intracontinental earthquakes (Kopnichev and Sokolova, 2013). We can suppose that this effect is related to relatively small variations in the mean rate of fluid migration at the stage of formation of ring-shaped structures (Kopnichev and Sokolova, 2013). At the same time, before this stage, fluids mainly migrate along faces of grains under the effect of shear stresses (Hier-Majumder and Kohlstedt, 2006), and these processes in continental regions run much more slowly when compared to the subduction zones (Kopnichev and Sokolova, 2013).

CONCLUSIONS

The practical value of the data from the present study is that they can be used to forecast locations and energies of the upcoming (preparing) large earthquakes from the characteristics of formed ring-shaped structures. Examples of such a forecast for the Tohoku earthquake of March 11, 2011, in northeast Japan and the Ikike earthquake of April 1, 2014, in Chile were given in (Kopnichev and Sokolova, 2009c, 2011a, 2015). Based on the analysis of parameters of seismicity rings formed 2 years before the Tohoku earthquake, it was concluded that a large (M_w ~ 8.7–8.9) earthquake was preparing to the east of Honshu Island (Kopnichev and Sokolova, 2009c), whereas Japanese seismologists believed that this region could not raise a subduction-related seismic events with $M_w > 8.3$ (Yamanaka and Kikuchi, 2004; Goldfinger et al., 2013). The magnitude estimate $M_w = 8.2 \pm 0.2$ obtained 4 years before the Ikike earthquake for the respective region corresponded to its real value; note that the epicenter of this earthquake was located near the intercept of the shallow and deep seismicity rings (Kopnichev and Sokolova, 2010, 2015). Of special interest is the possibility of predicting locations and magnitudes of the great earthquakes, with $M \geq 9.0$, for which recurrence intervals T_r can be many centuries (Goldfinger et al., 2013); predicting the intensity of expected tsunamis also relates to this problem.

Judging by the available data, the most reliable magnitude estimate for the western Pacific can be obtained from an analysis of M_{th1} and M_{th2} values. On the contrary, the same estimates for the eastern Pacific could also be based on the sizes of ring-shaped structures. Additionally, the current T_1 and T_2 values, probably can be used for midterm forecast of large earthquakes (which is especially important for earthquakes with M_w ~ > 9.0, for which the relations $T_r/T_1 \sim T_r/T_2 \gg 10$ can be satisfied), but, of course, the large scatter of values of these parameters should be taken into consideration.

REFERENCES

Abers, G., Nakajima, J., van Keken, P., Kita, S., and Hacker, B., Thermal-petrological controls on the location of earthquakes within subducting plates, *Mar. Geol.*, 2013, vols. 369–370, pp. 178–187.

Butler, R., Lay, T., Creager, K., et al., The global seismographic network surpasses its design goal, *EOS, Trans. Am. Geophys. Union*, 2004, vol. 85, no. 23, pp. 225–229.

Engdahl, E. and Villasenor, A., Global seismicity: 1990–1999, in *International Handbook of Earthquake and Engineering Seismology*, Elsevier, 2002, pp. 665–690.

Gold, T. and Soter, S., Fluid ascent through the solid lithosphere and its relation to earthquakes, *Pure Appl. Geophys.*, 1984/1985, vol. 122, pp. 492–530.

Goldfinger, C., Ikeda, Ya., Yeats, R., and Ren, J., Superquakes and supercycles, *Seismol. Res. Lett.*, 2013, vol. 84, no. 1, pp. 24–32.

Hier-Majumder, S. and Kohlstedt, D., Role of dynamic grain boundary wetting in fluid circulation beneath volcanic arcs, *Geophys. Res. Lett.*, 2006, vol. 33, L08305.

Husen, S. and Kissling, E., Postseismic fluid flow after the large subduction earthquake of Antofagasta, Chile, *Geology*, 2001, vol. 29, no. 9, pp. 847–850.

Karakin, A.V. and Lobkovskii, L.I., Hydrodynamics and the structure of two-phase asthenosphere, *Dokl. Akad. Nauk SSSR*, 1982, vol. 268, no. 2, pp. 324–329.

Kopnichev, Yu.F. and Sokolova, I.N., Spatiotemporal variations of the *S*-wave attenuation field in the source zones of large earthquakes in the Tien Shan, *Izv., Phys. Solid Earth*, 2003, vol. 39, no. 7, pp. 568–579.

Kopnichev, Yu.F. and Sokolova, I.N., Spatiotemporal variations of the S-wave attenuation field in source zones of strong earthquakes in the Tien Shan region: Evidence from the records of underground nuclear explosions, *Dokl. Earth Sci.*, 2004, vol. 395, no. 3, pp. 461–464.

Kopnichev, Yu.F. and Sokolova, I.N., Rise of mantle fluids in areas of sources of strong earthquakes and large fault zone: Geochemical evidence, *Vestn. NYaTs RK*, 2005, no. 2, pp. 147–155.

Kopnichev, Yu.F. and Sokolova, I.N., Ring seismicity in different depth ranges before large and great earthquakes in subduction zones, *Dokl. Earth Sci.*, 2009a, vol. 425, no. 2, pp. 448–450.

Kopnichev, Yu.F. and Sokolova, I.N., Characteristics of ring seismicity in different depth ranges before large and great earthquakes in the Sumatra region, *Dokl. Earth Sci.*, 2009b, vol. 429, no. 1, pp. 1385–1388.

Kopnichev, Yu.F. and Sokolova, I.N., Characteristics of ring seismicity in different depth ranges in the region of Northeast Japan, *Vestn. Nats. Yad. Tsentra Resp. Kaz.*, 2009c, no. 3, pp. 88–97.

Kopnichev, Yu.F. and Sokolova, I.N., On the correlation between seismicity characteristics and S-wave attenuation in the ring structures that appear before large earthquakes, *J. Volcanol. Seismol.*, 2010, vol. 4, no. 6, pp. 396–411.

Kopnichev, Yu.F. and Sokolova, I.N., Annular seismicity structures and the March 11, 2011, earthquake ($M_w = 9.0$) in Northeast Japan, *Dokl. Earth Sci.*, 2011a, vol. 440, no. 1, pp. 1324–1327.

Kopnichev, Yu.F. and Sokolova, I.N., Inhomogeneities in the field of short-period S-wave attenuation at the source of the Maule (Chili, February 27, 2010; $M_w = 8.8$) earthquake and their correlation with seismicity and the regional volcanism, *Geofiz. Issled.*, 2011b, vol. 12, no. 3, pp. 22–33.

Kopnichev, Yu.F. and Sokolova, I.N., Ring structures of seismicity generated in the continental areas before strong earthquakes with different source mechanisms, *Geofiz. Issled.*, 2013, vol. 14, no. 1, pp. 5–15.

Kopnichev, Yu.F. and Sokolova, I.N., Ring structures of seismicity in northern Chile and a successful forecast of the place and magnitude of the Iquique earthquake on April 1, 2014 ($M_w = 8.2$), *Vestn. Nats. Yad. Tsentra Resp. Kaz.*, 2015, no. 4, pp. 153–159.

Kopnichev, Yu.F., Gordienko, D.D., and Sokolova, I.N., Space–time variations of the shear wave attenuation field in the upper mantle of seismic and low seismicity areas, *J. Volcanol. Seismol.*, 2009, vol. 3, no. 1, pp. 44–58.

Letnikov, F.A., *Sinergetika geologicheskikh sistem* (Synergy of Geological Systems), Novosibirsk: Nauka, 1992.

Müller, R., Sdrolias, M., Gaina, C., and Roest, W., Age, spreading rates and spreading symmetry of the world's ocean crust, *Geochem. Geophys. Geosyst.*, 2008, no. 9, Q04006. doi 10.1029/2007GC001743

Ogawa, R. and Heki, K., Slow postseismic recovery of geoid depression formed by the 2004 Sumatra-Andaman earthquake by mantle water diffusion, *Geophys. Res. Lett.*, 2007, vol. 34, L06313. doi 10.1029/2007GL029340

Rojstaczer, S. and Wolf, S., Permeability changes associated with large earthquakes: An example from Loma Prieta, California, *Geology*, 1992, vol. 20, pp. 211–214.

Singh, S. and Suarez, G., Regional variation in the number of aftershocks ($mb \geq 5$) of large subduction-zone earthquakes ($M_w \geq 7.0$), *Bull. Seismol. Soc. Am.*, 1988, vol. 78, no. 1, pp. 230–242.

Tajima, F. and Kanamori, H., Global survey of aftershock area expansion, *Phys. Earth. Planet. Int.*, 1985, vol. 40, pp. 77–134.

Van'yan, L.L. and Hyndman, R.D., On the origin of electrical conductivity in the consolidated crust, *Izv., Phys. Solid Earth*, 1996, no. 4, pp. 268–284.

Yamanaka, Y. and Kikuchi, M., Asperity map along the subduction zone in northeast Japan inferred from regional seismic data, *J. Geophys. Res.*, 2004, vol. 109, B07307. doi 10.1029/2004JB003203

Yamazaki, T. and Seno, T., Double seismic zone and dehydration embrittlement of the subducting slab, *J. Geophys. Res.*, 2003, vol. 108, no. B4. doi 10.1029/2002JB001918

Translated by N. Astafiev